Am J Physiol Gastrointest Liver Physiol 313: G353–G360, 2017.
First published June 15, 2017; doi:10.1152/ajpgi.00169.2017.

RESEARCH ARTICLE | *Nutrient Sensing, Nutrition, and Metabolism*

Consumption of a high-iron diet disrupts homeostatic regulation of intestinal copper absorption in adolescent mice

Jung-Heun Ha, Caglar Doguer, and James F. Collins

Food Science and Human Nutrition Department, University of Florida, Gainesville, Florida

Submitted 24 May 2017; accepted in final form 12 June 2017

Ha JH, Doguer C, Collins JF. Consumption of a high-iron diet disrupts homeostatic regulation of intestinal copper absorption in adolescent mice. *Am J Physiol Gastrointest Liver Physiol* 313: G353–G360, 2017. First published June 15, 2017; doi:10.1152/ajpgi.00169.2017.—High-iron feeding of rodents has been commonly used to model human iron-overload disorders. We recently noted that high-iron consumption impaired growth and caused severe systemic copper deficiency in growing rats, but the mechanism by which this occurred could not be determined due to technical limitations. In the current investigation, we thus utilized mice; first to determine if the same phenomenon occurred in another mammalian species, and second since we could assess in vivo copper absorption in mice. We hypothesized that excessive dietary iron impaired intestinal copper absorption. Weanling, male mice were thus fed AIN-93G-based diets containing high (HFe) (~8,800 ppm) or adequate (AdFe) (~80 ppm) iron in combination with low (~0.9 ppm), adequate (~9 ppm), or high (~180 ppm) copper for several weeks. Iron and copper homeostasis was subsequently assessed. Mice consuming the HFe diets grew slower, were anemic, and had lower hepatic copper levels and serum ceruloplasmin activity. These physiological perturbations were all prevented by higher dietary copper, demonstrating that copper depletion was the underlying cause. Furthermore, homeostatic regulation of copper absorption was noted in the mice consuming the AdFe diets, with absorption increasing as dietary copper decreased. HFe-fed mice did not have impaired copper absorption (disproving our hypothesis), but homeostatic control of absorption was disrupted. There were also noted perturbations in the tissue distribution of copper in the HFe-fed mice, suggesting that altered storage and thus bioavailability contributed to the noted copper deficiency. Dietary iron loading thus antagonizes copper homeostasis leading to pathological symptoms of severe copper depletion.

NEW & NOTEWORTHY High-iron feeding is a common experimental method to model human iron-overload disorders in rodents. Here, we show that dietary iron loading causes severe copper deficiency due to perturbations in the homeostatic regulation of intestinal copper absorption and tissue distribution, which may decrease the bioavailability of copper for use in cuproenzyme synthesis. Whether high-dose iron supplementation in humans antagonizes copper homeostasis is worthy of consideration.

iron loading; copper-deficiency anemia; erythropoietin; copper absorption and distribution

IRON AND COPPER are essential trace minerals for mammals, and given their similar physiochemical properties, numerous physiologically relevant interactions between them have been documented over the past several decades (4, 5, 11). Our recent studies, and those of numerous others, have begun to elucidate the molecular mechanisms by which copper influences iron homeostasis. Iron deficiency in rodents causes upregulation of an intestinal copper transporter (Atp7a) involved in cuproenzyme synthesis and copper export from enterocytes (3, 10, 22), which led us to the logical postulate that copper positively influences intestinal iron transport. Moreover, a basolaterally expressed intestinal ferroxidase, hephaestin, is a copper-dependent protein which is necessary for optimal iron absorption (7), especially during pregnancy and the immediate postweaning period (C. Doguer, J. H. Ha, S. Gulec, C. D. Vulpe, G. J. Anderson, and J. F. Collins, unpublished observations). A circulating copper-dependent protein, ceruloplasmin (Cp), with homology to hephaestin and a conserved ferroxidase function, also exemplifies another link between iron and copper (5, 15). Furthermore, iron depletion alters copper distribution, including increasing hepatic copper content, whereas copper depletion leads to hepatic iron accumulation (5, 11). More recently, we noted that high-iron feeding of growing rats led to copper depletion and associated symptoms of copper deficiency, including cardiac hypertrophy, growth retardation, and severe anemia [in the setting of hyperferremia] (13). In this latter study, the mechanism by which dietary iron overload caused copper deficiency was, however, not determined. The current investigation was thus undertaken to test the hypothesis that high dietary iron inhibits intestinal copper absorption. Precedence for such interactions among dietary minerals is well established. We also sought to confirm these iron-copper interactions in another mammalian species (i.e., mice). This investigation demonstrated that, as in rats, high dietary iron caused copper depletion, and moreover, that dietary iron overload disrupted homeostatic control of intestinal copper absorption and tissue distribution.

MATERIALS AND METHODS

Animal experiments. All animal studies were approved by the University of Florida IACUC. Three-week-old male, weanling C57BL/6 mice (Jackson Laboratories; Bar Harbor, ME) were housed in stainless steel, overhanging, wire mesh-bottom cages to minimize coprophagia. Mice had ad libitum access to chow and purified water. Semi-purified diets (Dyets; Bethlehem, PA) were based on the AIN-93G formulation and contained high (~8,800 ppm) or adequate (~80 ppm) iron in combination with high (~180 ppm), adequate (~9 ppm), or low ~(0.9 ppm) copper (Tables 1, 2, and 3). All diets were identical to those used in our previous study in rats (13), and varied only in iron and copper content. Experimental mice were weighed weekly and food consumption was estimated by weighing the amount of food

Address for reprint requests and other correspondence: J. F. Collins, Food Science & Human Nutrition Department, Univ. of Florida, 441 FSN Building, PO Box 110370, Newell Dr., Gainesville, FL 32611-0370 (e-mail: jfcollins@ufl.edu).

 0193-1857/17 Copyright © 2017 the American Physiological Society

Downloaded from http://ajpgi.physiology.org/ by 10.220.33.6 on November 6, 2017

Table 1. *Iron and copper concentrations in experimental diets*

Diet	Fe, ppm*	Cu, ppm*
AdFe/LCu	93.7	0.92
AdFe/AdCu	71.9	8.96
AdFe/HCu	71.8	183
HFe/LCu	9,036	0.94
HFe/AdCu	8,707	9.18
HFe/HCu	8,718	184

H, high; Ad, adequate; L, low. *Determined by ICP/MS.

provided daily to each cage of mice. Mice were euthanized by CO_2 inhalation followed by thoracotomy. For all animal experiments, including ^{64}Cu absorption and distribution experiments, mice were fed the experimental diets for 5 wk, fasted overnight (~16 h) but allowed free access to purified water, and then administered a copper transport solution (20 μCi ^{64}Cu diluted in PBS containing 0.1 N HCl) by oral gavage. ^{64}CuCl (39.4 mCi/mg) was obtained from Washington University (St. Louis, MO). After gavage, mice were immediately given ad libitum access to the same diets and water, and then euthanized 8–9 h later. This time point was selected since intestinal transit time in mice is ~11 h (1) and mice can excrete copper in bile. Also, the half-life of ^{64}Cu (12.7 h) necessitates a shorter experimental period. Radioactivity was measured using a WIZARD^2 Automatic Gamma Counter (Perkin Elmer; Waltham, MA) and corrected for the half-life of ^{64}Cu. ^{64}Cu absorption was calculated as a ratio of counts per minute (cpm) in the carcass (minus the entire GI tract) to total cpm administered by gavage multiplied by 100. Radioactivity in blood was expressed as cpm per microliter and radioactivity in tissues as cpm per milligram wet weight.

Hematological parameters, serum and tissue iron quantification, and Cp activity. Hemoglobin (Hb) and hematocrit (Hct) were quantified using standard techniques, as described by us previously (13). Quantification of nonheme serum and hepatic iron, total iron-binding capacity (TIBC), and transferrin (Tf) saturation levels was also done using standard methodologies (10, 13). Cp possesses amine oxidase activity, which can be utilized to determine Cp activity in serum. An amine oxidase [*para*-phenylenediamine (*p*PD)] assay was performed by a previously reported method (13, 20).

Determination of iron and copper concentrations in diets and tissues. Diet samples (from 10 randomly selected pellets) were digested with HNO_3/H_2O_2 using the US Environmental Protection Agency Method 3050B (25) on a hot block (Environmental Express; Charleston, SC). Digested diets were filtered (0.45 μm) and analyzed by inductively-coupled plasma mass spectrometry (ICP-MS) (NexIon 300, Perkin-Elmer; Norwalk, CT). Tissue samples were digested with HNO_3 (95°C) overnight and diluted in purified water and analyzed by flame atomic absorption spectrometry (AAS) (AAnalyst 100, Perkin-Elmer; Waltham, MA). Mineral concentrations in tissues were normalized by tissue weights.

Table 2. *Constant ingredients in the 6 experimental diets*

Ingredient	Amount, g/kg
Casein	200
Sucrose	100
Soybean oil	70
t-Butyhydroquinone	0.014
Dyetose	132
Cellulose (micro)	50
Mineral Mix	35
Vitamin Mix	10
Choline bitartrate	2.5
L-Cystine	3

Table 3. *Variable ingredients in the 6 experimental diets*

Ingredient	AdFe/LCu	AdFe/AdCu	AdFe/HCu	HFe/LCu	HFe/AdCu	HFe/HCu
Cornstarch, g/kg	397.486	397.486	397.486	387.486	387.486	387.486
Fe Premix (10 mg/g)	8	8	8	0	0	0
Carbonyl Fe, g/kg	0	0	0	10	10	10
Cu Premix (1 mg/g)	0.5	0	0	0.5	0	0
Cu Premix (5 mg/g)	0	1.6	40	0	1.6	40
Kilocalories per kg	3,760	3,760	3,760	3,724	3,724	3,724

qRT-PCR. Total RNA was isolated using RNAzol RT reagent (Molecular Research Center, Cincinnati, OH) and SYBR Green qRT-PCR was subsequently performed, as described in detail previously (13). Oligonucleotide primers (Table 4) were designed to span large introns to avoid amplification from genomic DNA. Expression of each experimental gene was normalized to the expression of cyclophilin. Mean fold changes in mRNA expression were calculated by the $2^{-\Delta\Delta Ct}$ analysis method.

Statistical analysis. Statistical analyses were performed using GraphPad Prism (version 7.0.1 for Windows) with critical significance level $\alpha = 0.05$. Data are presented as arithmetic means and standard deviation (SD) for *n* independent observations, or as box plots [displaying the minimum, the lower (25th percentile), the median (50th percentile), the upper (75th percentile), and the maximum ranked sample]. Renal Epo mRNA data were analyzed after $\log_{10}$ transformation due to unequal variance. Inferences were made using appropriate statistical tests as indicated in the figure legends. In some cases, to understand the relationship between two variables, Pearson product-moment correlation coefficient (*r*) was calculated.

RESULTS

High-iron feeding causes physiological perturbations that are largely prevented by increasing dietary copper content. Mice consuming the AdFe diets were of similar size at euthanasia, and growth rates were the same over the 5-wk feeding period, regardless of dietary copper levels (Fig. 1*A*). Mice consuming the HFe diets, however, were smaller than mice consuming the AdFe diets at euthanasia. Increasing copper in the HFe diets led to a trend of increasing body size toward control values (i.e., the AdFe/AdCu group) (Fig. 1*A*). Consumption of the HFe/LCu diet decreased growth rates, but growth was restored with increasing copper levels in the HFe diets (Fig. 1*B*). Importantly, growth deficits were not the result of decreased energy (kcal) intake, as food consumption was not different between experimental groups (data not shown), and the energy content of the different diets varied by <1%. Furthermore, high-iron feeding with low copper caused cardiac hypertrophy, but progressively increasing the copper content in the HFe diets reduced heart size to normal (Fig. 1*C*). Consumption of the HFe/LCu diet also caused mortality in some mice, whereas adding more copper to the HFe diets reduced (AdCu) or prevented (HCu) premature death (Fig. 1*D*). These data demonstrate that high-iron consumption antagonizes copper homeostasis, thus leading to well-established physiological perturbations associated with copper depletion, including

Table 4. *qRT-PCR primer sequences (5′ to 3′)*

Transcript	Forward	Reverse
Cyclophilin	CTTACGACAAGCAGCCCTTCATG	AGCTGTTTTTAACTCACTGCTGTTGTA
Epo	ATGAAGACTTGCAGCGTGGA	AGGCCCAGAGGAATCAGTAG
Hepc	GCCCTTCAGGAACAGCTATG	ACTGGTCTGTTGTGGGTGGT

Downloaded from http://ajpgi.physiology.org/ by 10.220.33.6 on November 6, 2017

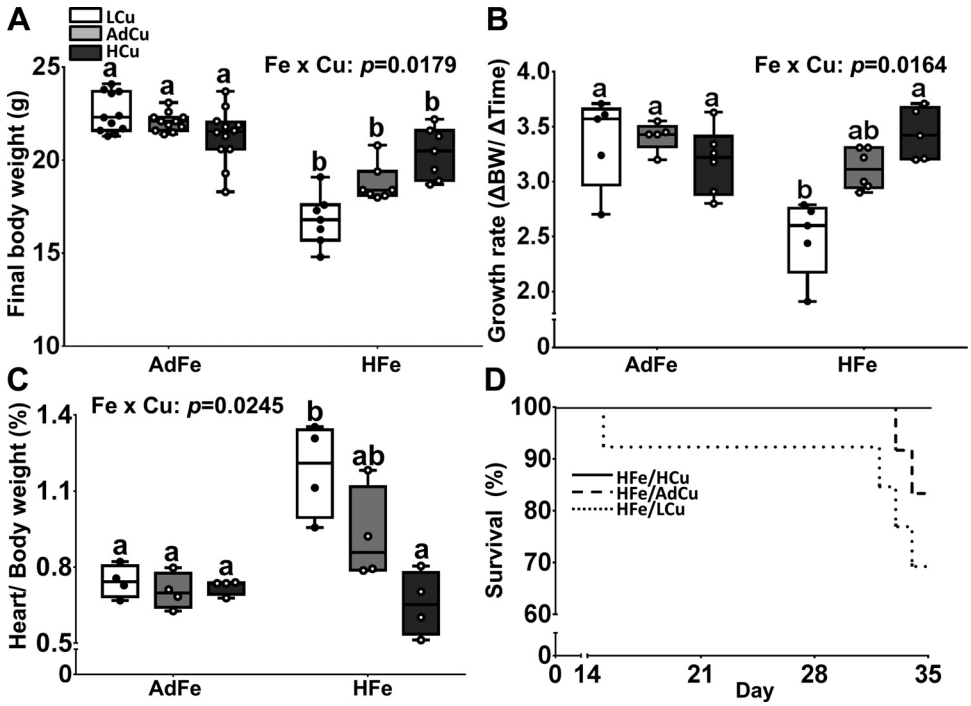

Fig. 1. High-iron consumption impaired growth, caused cardiac hypertrophy, and increased mortality, but higher dietary copper prevented these abnormalities. Weanling C57BL/6 mice were fed 1 of 6 diets varying only in iron and copper content for 5 wk ad libitum. Final body weight (*A*) and growth rates (*B*) were subsequently determined. Heart weight normalized to body weight (*C*) was also determined at euthanasia. Data are presented as box plots representing 4 (heart weight) or 7–12 (final body weight and growth rate) mice per group. Data were analyzed by 2-way ANOVA on ranks analysis. Significant iron main effects were noted for final body weights ($P < 0.0001$), growth rates ($P = 0.0019$), and heart weights ($P = 0.0097$). A copper main effect was also noted in regard to heart weights ($P = 0.0115$). Two-way Fe × Cu interactions were also noted (as indicated in *A*–*C*). Since significant 2-way interactions were observed, Tukey's multiple comparisons post hoc test was utilized to determine differences among individual groups for each parameter; labeled means without a common letter differ ($P < 0.05$). Mortality (*D*) was also monitored since some mice died during the 5-wk feeding trial ($n = 12$ per group). L, low; Ad, adequate; H, high. Note that these same abbreviations are used in all figures.

growth impairment, cardiac hypertrophy, and increased mortality (4, 11, 19).

High-iron consumption disrupts copper homeostasis. Consumption of the LCu/AdFe diet caused anemia in growing mice, which was an anticipated result (Fig. 2, *A* and *B*) (5). Unexpectedly, consumption of the high-iron diet led to more severe anemia; adding extra copper to the HFe diet, however, prevented the noted decreases in Hb and Hct. Interestingly, altering the copper content of both the AdFe and HFe diets led to alterations in serum nonheme iron, with opposing effects (Fig. 2*C*). That is, higher copper in the AdFe diets progressively increased serum nonheme iron content, whereas, conversely, higher copper in the HFe diets decreased serum nonheme iron levels. TIBC was similar between all of the dietary treatment groups (Fig. 2*D*). Increases in copper content in the AdFe diet led to a trend toward increased Tf saturation ($P = 0.06$), and Tf saturation was higher in all of the HFe groups (Fig. 2*E*). Furthermore, renal Epo expression was higher in the LCu/HFe and AdCu/HFe groups, but expression was normalized by higher copper in the HFe diet (Fig. 2*F*). We previously reported that renal Epo mRNA expression accurately reflected circulating hormone levels in rats (13). Collectively, these data demonstrate that high-iron feeding leads to copper-deficiency anemia. Moreover, dietary copper differentially influences serum nonheme iron concentrations and transferrin saturation under basal and iron-loaded conditions.

Excess dietary copper potentiates hepatic iron loading in response to high-iron feeding. Hepcidin (Hepc) blocks iron export via ferroportin 1 (Fpn1) in intestinal enterocytes and reticuloendothelial (RE) macrophages of the spleen, bone marrow, and liver, thus decreasing serum iron (12, 23). Hepc expression is also an excellent indicator of body iron status. We thus quantified hepatic Hepc mRNA levels in our experimental mice. High-iron feeding increased hepatic Hepc mRNA expression to a similar extent in all three dietary copper groups (Fig. 3*A*). Moreover, Hepc expression correlated with serum Tf saturation (Fig. 3*B*); increased Tf saturation stimulates *Hamp* (encoding Hepc) transcription (8, 13, 26). Furthermore, given that liver iron stores reflect whole body iron status, hepatic nonheme iron was quantified. Liver iron content was much higher in mice consuming the HFe diets, with higher dietary copper causing more significant hepatic iron loading (Fig. 3*C*). Hepatomegaly was also observed in mice consuming the HFe diets (Table 5), consistent with known manifestations of liver iron loading (2, 24). Furthermore, hepatic nonheme iron content correlated with Hepc mRNA expression (Fig. 3*D*), consistent with the known influence of body iron stores on *Hamp* gene transcription (8, 18). These data demonstrate that high-iron feeding caused hepatic iron loading, despite high Hepc expression, suggesting that the mechanism of iron loading in this dietary model does not depend upon iron export from duodenal enterocytes via Fpn1. We speculate that intestinal

Downloaded from http://ajpgi.physiology.org/ by 10.220.33.6 on November 6, 2017

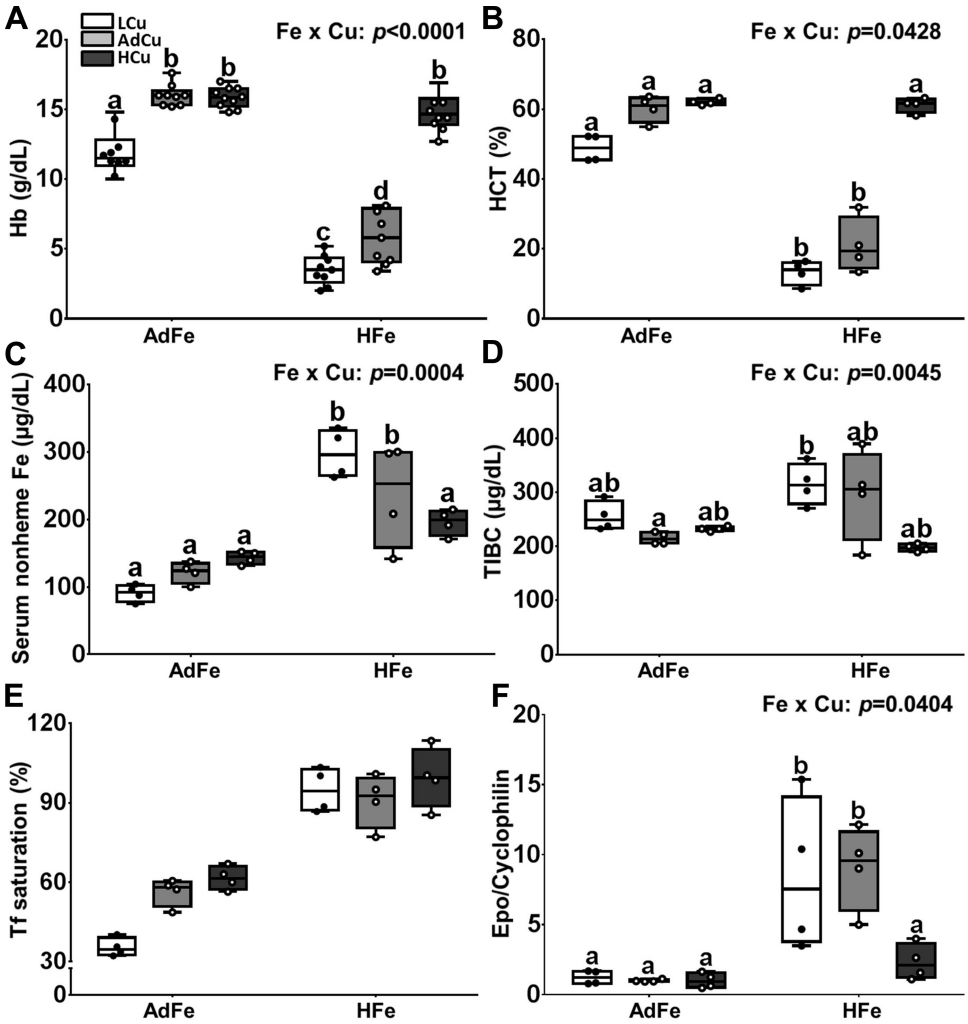

Fig. 2. High-iron consumption caused anemia and increased renal Epo expression, but extra dietary copper prevented these physiological perturbations. Weanling C57BL/6 mice were fed 1 of 6 diets varying only in iron and copper content for 5 wk ad libitum. Hemoglobin (Hb) (*A*) and hematocrit (HCT) (*B*) levels were determined at euthanasia, along with serum nonheme iron (*C*), total iron-binding capacity (TIBC) (*D*), and transferrin (Tf) saturation (*E*). Renal erythropoietin (Epo) mRNA expression was also quantified by qRT-PCR analysis (*F*). Data are presented as box plots representing 9–11 (Hb) or 4 (all others) mice per group. Two-way ANOVA on ranks analysis revealed an iron main effect for Hb and Hct levels, serum nonheme Fe concentrations, Tf saturation, and Epo mRNA expression ($P < 0.0004$ for all). A copper main effect was also noted in regard to Hb and Hct levels, TIBC, and Epo mRNA expression ($P < 0.0079$ for all). Two-way Fe × Cu interactions were also noted for all measured parameters except Tf saturation (as indicated in *A–D* and *F*). Since significant 2-way interactions were noted, Tukey's multiple comparisons post hoc test was utilized to determine differences among individual groups for each parameter; labeled means without a common letter differ ($P < 0.05$). Data for Epo mRNA expression were $\log_{10}$ transformed before running statistical analyses; however, for ease of interpretation, the nontransformed data are depicted in the figure (*F*).

iron flux occurs via the paracellular pathway when dietary iron levels are excessive.

High-iron consumption perturbs hepatic copper homeostasis. Given that extra dietary copper corrected many of the pathological abnormalities associated with high-iron consumption, we next assessed liver copper levels and serum Cp activity. Hepatic copper levels were low in the HFe groups, except for in the HFe/HCu group in which liver copper was the same as controls (Fig. 4*A*). Serum Cp activity was depressed in the AdFe/LCu group and also in the HFe groups with low and adequate copper (Fig. 4*B*). Again, the extra copper in the HFe diet prevented the decrement in Cp activity. Furthermore, serum Cp activity correlated with liver copper content (Fig. 4*C*), consistent with the postulate that higher liver copper leads to increased production of *holo*-Cp (the active, copper-containing enzyme) (21). These data thus provide additional evidence that dietary iron overload antagonizes copper homeostasis.

Homeostatic regulation of copper absorption is perturbed by high dietary iron. Since high-iron feeding led to systemic copper deficiency, we postulated that intestinal copper absorption was impaired. Radiotracer ^{64}Cu uptake studies were thus performed. The experimental approach was to gavage mice with the ^{64}Cu uptake solution, immediately followed by providing the fasted mice ad libitum access to chow and water. Absorption was thus assessed in the setting of a normal meal, giving the experimental approach physiological relevance. In the AdFe groups, copper (^{64}Cu) absorption varied by dietary copper levels; absorption was highest in the LCu group (>50% of the administered ^{64}Cu dose), intermediate in the AdCu group (~30%), and lowest in the HCu group (~10%) (Fig. 5*A*). Blood and tissue ^{64}Cu accumulation in the AdFe groups reflected absorption as the same pattern was observed without exception (Fig. 5, *B–I*). In the high-iron-fed mice, this homeostatic control of copper absorption and distribution was disrupted. This was exemplified by the observations that copper absorption was not increased in the HFe/LCu and HFe/AdCu groups (despite severe copper deficiency), and copper absorption was not downregulated in the HFe/HCu group (Fig. 5*A*). Copper absorption in all the HFe groups was, in fact, comparable to the control group (i.e., the AdFe/AdCu group) (20–30% of the ^{64}Cu dose). Despite similar copper absorption, tissue ^{64}Cu accumulation was lower in all the HFe groups, being most similar to the AdFe/HCu group (Fig. 5, *B–I*). Focusing on the AdCu groups provides clarity on the dysregulation of copper homeostasis in the iron-loaded mice. Copper absorption (whole body radioactivity minus the GI tract) was similar in controls (i.e., the AdFe/AdCu group) and the HeFe/AdCu group, yet copper accumulation was lower in every

Downloaded from http://ajpgi.physiology.org/ by 10.220.33.6 on November 6, 2017

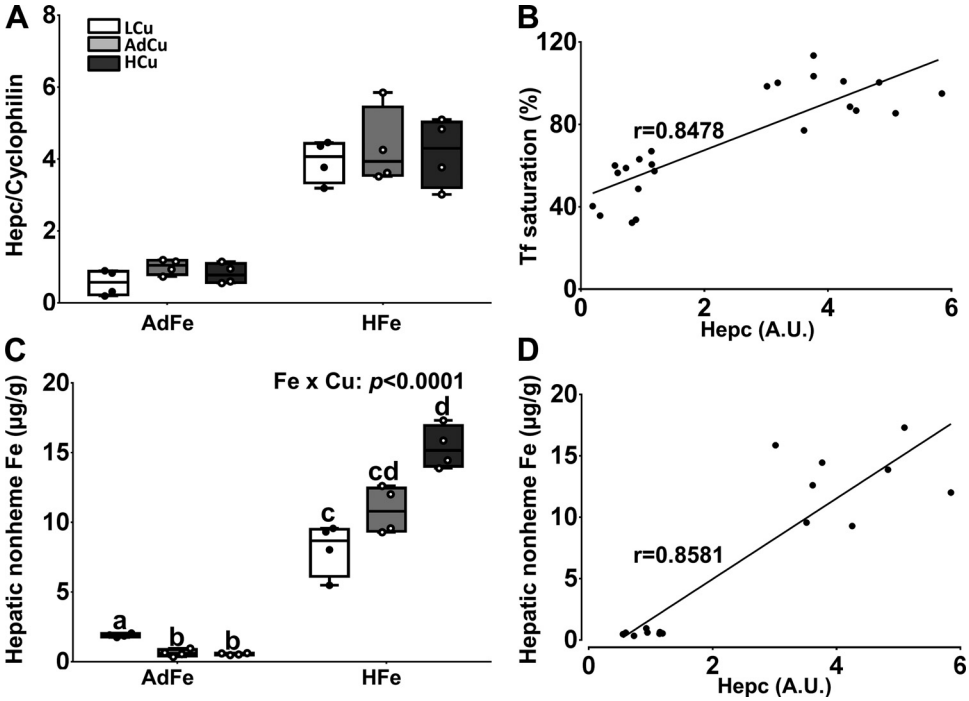

Fig. 3. Variations in copper intake alter hepatic iron loading caused by high-iron consumption. Weanling C57BL/6 mice were fed 1 of 6 diets varying only in iron and copper content for 5 wk ad libitum. Hepc mRNA expression was quantified by qRT-PCR (*A*). Hepatic nonheme iron was measured using a standard spectrophotometric method (*C*). Data are presented as box plots representing 4 mice per group. Two-way ANOVA on ranks analysis revealed an iron main effect for Hepc mRNA expression ($P < 0.0001$) and hepatic nonheme iron concentrations ($P < 0.0001$). A two-way Fe × Cu interaction was noted for hepatic nonheme iron levels (as indicated in *C*). Since a significant 2-way interaction was observed, Tukey's multiple comparisons post hoc test was utilized to determine differences among individual groups; labeled means without a common letter differ ($P < 0.05$). Furthermore, the relationships between Hepc mRNA expression and Tf saturation (*B*) and hepatic nonheme iron levels (*D*) were assessed by calculating Pearson product-moment correlation. The lines of best fit are shown along with the correlation coefficients (r) ($P < 0.0001$).

tissue examined in the HFe group. This means that copper accumulated in other tissues that were not examined, or that copper excretion was increased. Overall, these data then suggest that high-iron consumption in the setting of high serum non-transferrin-bound iron (NTBI) and tissue iron loading perturbs homeostatic regulation of copper absorption, tissue distribution, and utilization.

DISCUSSION

Diets containing 1–3% carbonyl iron have been routinely used to create iron overload models. When these diets are consumed by rodents, hepatic Hepc expression is induced, which would normally limit intestinal iron absorption (6, 9). With this extreme level of dietary iron, however, physiological mechanisms which attenuate iron absorption are ineffective, and excessive dietary iron enters the portal blood and pathological tissue iron accumulation ensues. This method of iron loading models what has been referred to as "secondary" iron overload, in contrast to primary iron-loading disorders (e.g., hereditary hemochromatosis), which are genetic diseases that are typified by inappropriately low expression of Hepc (for a given body iron load). Since Hepc expression is high with dietary iron overload, iron initially accumulates in macrophages of the reticuloendothelial system, as iron export from these cells is impaired (due to Hepc-mediated Fpn1 degradation). Despite this, non-transferrin-bound iron (NTBI) eventually appears in the plasma and patterns of tissue iron loading are similar to those observed in hemochromatosis.

Table 5. *Organ weights (%body wt)*

Organ	AdFe/LCu	AdFe/AdCu	AdFe/HCu	HFe/LCu	HFe/AdCu	HFe/HCu
Liver*	5.36 ± 0.42	5.64 ± 0.61	4.96 ± 0.69	6.40 ± 0.42	6.80 ± 0.81	6.67 ± 0.67
Kidney	0.79 ± 0.07	0.83 ± 0.02	0.77 ± 0.04	0.88 ± 0.10	0.80 ± 0.06	0.83 ± 0.11
Spleen	0.41 ± 0.05	0.40 ± 0.02	0.37 ± 0.03	0.32 ± 0.08	0.44 ± 0.10	0.39 ± 0.08

Values are means ± SD; $n = 4$ per group. Data were analyzed by 2-way ANOVA. *Iron main effect ($P < 0.0001$).

In a survey of the literature, it was noted that high-iron feeding of growing rodents led to decreases in body weights in several studies (Table 6). This was associated with increases in liver and serum iron in some studies. The mechanism by which high-iron consumption impaired growth was not, however, experimentally established in any of these previous investigations. We also previously noted that high-iron feeding impaired growth in adolescent rats (13). Due to a fortuitous experimental design, we were able to demonstrate that increasing dietary copper intake prevented the growth defects caused by high-iron consumption. Moreover, several other symptoms typical of copper deficiency were prevented by increasing dietary copper intake, proving that consumption of the high-iron diet caused copper depletion (13). This observation is in fact consistent with a previous study in which rats were fed a high-iron diet with marginal copper content, leading to copper depletion (17). The mechanism by which high dietary iron antagonizes copper homeostasis, however, remains unknown. We postulated that excessive dietary iron could block copper transport in the gut, given the similar physiochemical properties of these trace minerals. The current investigation was thus undertaken to test the hypothesis that high-iron feeding impairs intestinal copper absorption. Mice were used for this investigation for two reasons: *1*) we sought to extend our previous observations in rats to another mammalian species; and *2*) intestinal copper (^{64}Cu) absorption experiments were feasible in mice, but not in rats (due to size limitations of the whole body gamma counter to which we have access).

Weanling mice fed the high-iron diet with low or adequate copper content for several weeks grew slower and had enlarged hearts. They were also copper depleted as exemplified by decreased hepatic copper concentrations and reduced serum Cp activity. Mice in these dietary groups also developed severe

Downloaded from http://ajpgi.physiology.org/ by 10.220.33.6 on November 6, 2017

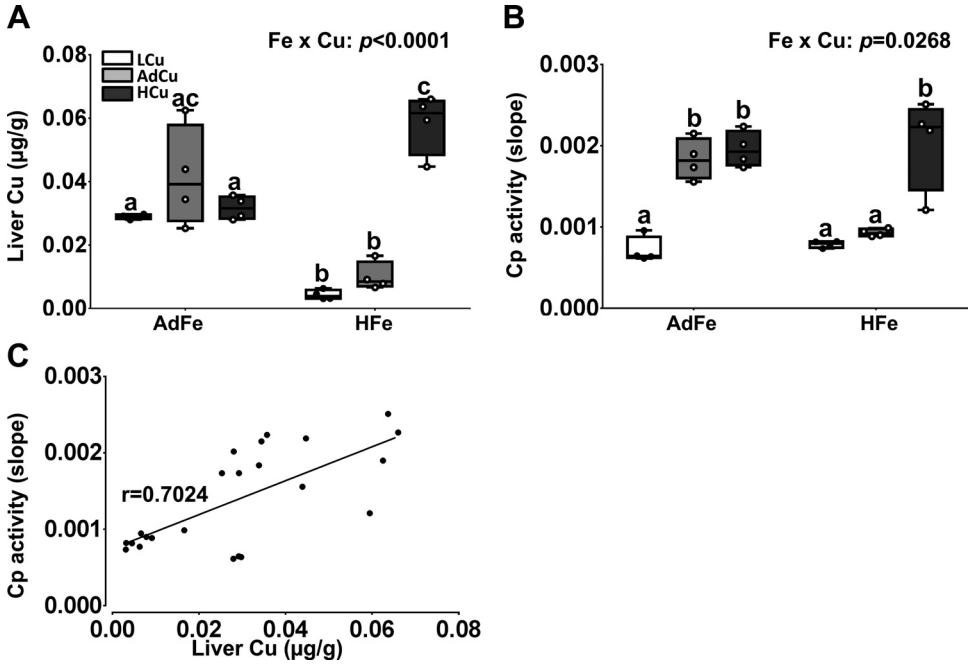

Fig. 4. High-iron consumption perturbs copper homeostasis. Weanling C57BL/6 mice were fed 1 of 6 diets varying only in iron and copper content for 5 wk ad libitum. Hepatic copper concentrations were quantified by AAS (*A*). Cp (i.e., amine oxidase) activity (*B*) was measured in serum samples using a spectrophotometric method. Data are presented as box plots representing 4 mice per group. Two-way ANOVA on rank analysis revealed an iron main effect for liver copper concentrations ($P = 0.0027$). A copper main effect was also noted in regard to liver copper content and serum Cp activity ($P < 0.0001$ for both). Two-way Fe × Cu interactions were also noted for both measured parameters (as indicated in *A* and *B*). Since significant 2-way interactions were noted, Tukey's multiple comparisons post hoc test was utilized to determine differences among individual groups for each parameter; labeled means without a common letter differ ($P < 0.05$). Furthermore, the correlation between Cp activity and liver copper concentrations was assessed using Pearson product-moment correlation analysis (*C*). The line of best fit is shown along with the correlation coefficient (r) ($P < 0.0001$).

anemia, as indicated by large decreases in serum Hb, Hct, and induction of renal Epo expression. This anemia developed in the setting of high serum Tf saturation, suggesting that iron utilization by developing erythrocytes was impaired (since these cells acquire iron via diferric Tf). This is, in fact, consistent with the postulate that copper is required for iron import into mitochondria or for heme synthesis in erythroblasts (5, 14), but the exact mechanism by which copper depletion causes iron-deficiency (-like) anemia is unknown. Importantly, all of these physiological perturbations were prevented by adding extra copper to the HFe diets.

Notably, variations in dietary copper were associated with altered blood and liver iron levels. For example, there was a reciprocal relationship between dietary copper levels and serum nonheme iron concentrations in the HFe groups ($r = 0.6772$). That is, lower dietary copper was associated with higher serum nonheme iron levels, and vice versa. This pattern was opposite to that of hepatic nonheme iron levels, which increased in parallel with dietary copper content. Thus, in the iron-loaded mice, high serum nonheme iron levels occurred when liver nonheme iron stores were lower, and as dietary copper intake increased, liver iron stores went up and serum iron levels went down. The mechanism by which alterations in copper intake influence iron homeostasis are unknown, but this phenomenon probably does not involve Hepc, since its expression was uniformly induced in all high-iron-fed mice. Moreover, changes in serum nonheme iron likely reflect NTBI, since Tf saturation and TIBC (which is a measure of the amount of circulating Tf) did not vary among the HFe groups.

In vivo copper absorption studies clearly demonstrated that mice consuming adequate iron levels have the ability to regulate copper absorption according to dietary copper levels. Lower copper intake was associated with higher absorption, and vice versa. This observation was affirmed by the similar pattern of ^{64}Cu appearance in blood and accumulation in numerous tissues. Strikingly, however, this homeostatic regulation of copper absorption was perturbed in the iron-loaded mice. Mice in the HFe groups all absorbed similar levels of copper, regardless of dietary copper levels, yet ^{64}Cu accumulation in all tissues examined was extremely low. So, mice consuming the HFe diet absorbed copper apparently normally (based upon total radioactivity in the carcass), but copper utilization was impaired in the low and adequate copper-fed groups (given their copper-deficiency-related pathologies). Moreover, even though we assessed copper accumulation in numerous tissues, we did not identify the location of the majority of the ^{64}Cu absorbed in the radioisotope tracer uptake experiments.

In summary, this investigation has demonstrated that growing mice fed a high-iron diet develop copper-deficiency anemia, which is accompanied by several pathological perturbations consistent with systemic copper deficiency. These findings extend our previous studies in rats to another mammalian species, increasing the potential physiological significance of these observations. Moreover, in vivo absorption studies showed that iron loading perturbs the homeostatic regulation of dietary copper absorption and also impairs copper distribution among different tissues. How high dietary iron consumption antagonizes copper homeostasis is unknown, but these experiments may have implications for humans who regularly take high-dose iron supplements, as has been previously suggested (16, 17). Additional experimentation is required to elucidate the molecular mechanisms by which dietary iron loading alters copper absorption, distribution, storage, and bioavailability.

ACKNOWLEDGMENTS

Present address of C. Doguer: Nutrition and Dietetics Dept., Namik Kemal Univ., Tekirdag, Turkey.

GRANTS

This investigation was funded by National Institute of Diabetes and Digestive and Kidney Diseases Grants R01-DK-074867 and R01-DK-109717 (to J. F. Collins).

Downloaded from http://ajpgi.physiology.org/ by 10.220.33.6 on November 6, 2017

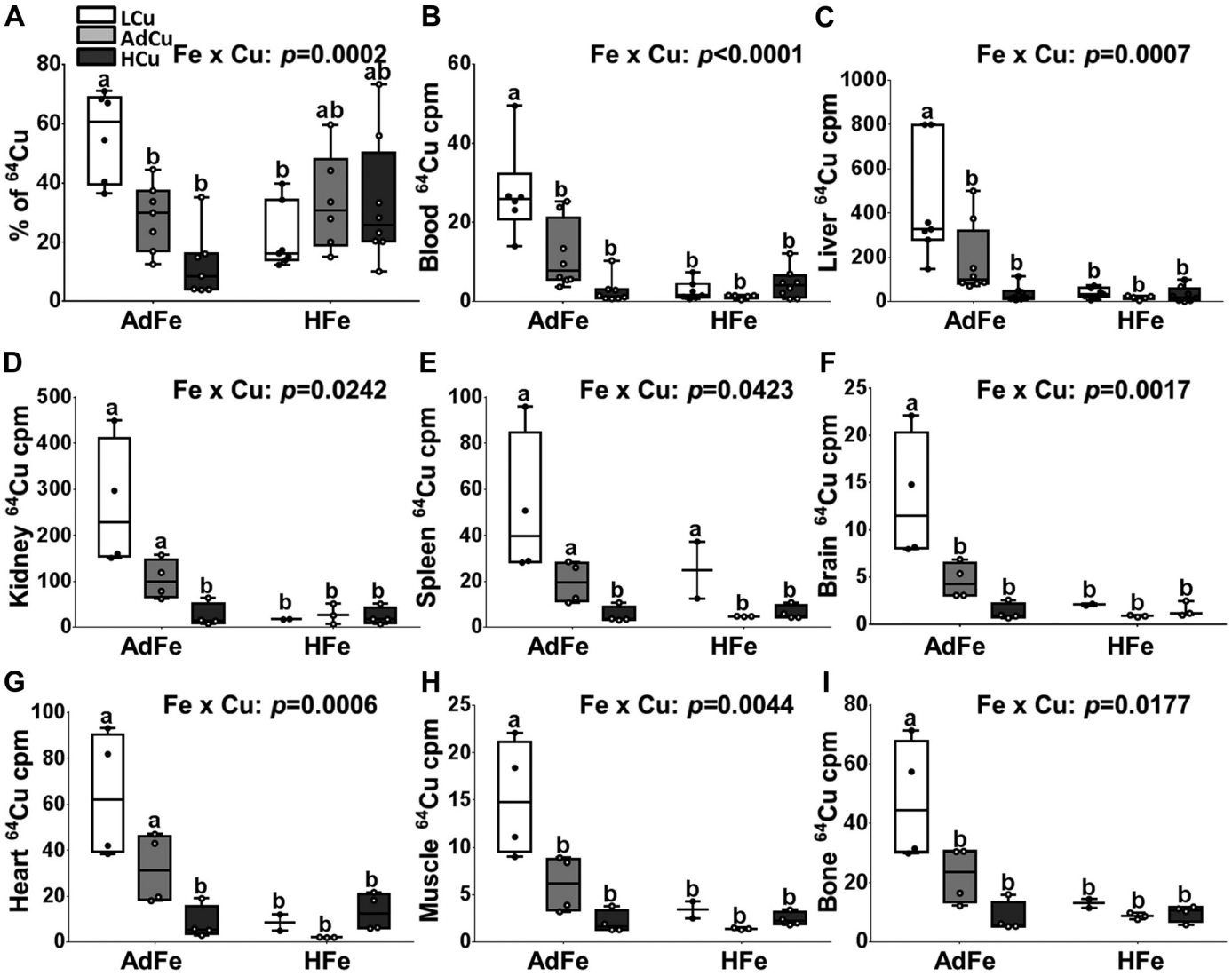

Fig. 5. High-iron consumption perturbed ^{64}Cu absorption and tissue distribution. Weanling C57BL/6 mice were fed 1 of 6 diets varying only in iron and copper content for 5 wk ad libitum. Subsequent to the dietary regimen, copper absorption and tissue distribution were determined after oral gavage of ^{64}Cu. ^{64}Cu absorption (percent) (*A*), and distribution in blood (*B*), liver (*C*), kidney (*D*), spleen (*E*), brain (*F*), heart (*G*), muscle (tibialis anterior) (*H*), and bone (tibia) (*I*) were determined by gamma counting and values were normalized by volume (blood) or weight (tissues) of specimens. Data are presented as box plots representing 6–8 (*A–C*) or 2–4 (*D–I*) mice per group. Two-way ANOVA on ranks analysis revealed an iron main effect for ^{64}Cu content in blood, liver, kidney, brain, heart, muscle, and bone ($P < 0.0084$ for all). A copper main effect was also noted in regard to ^{64}Cu absorption and ^{64}Cu accumulation in all tissues except heart ($P < 0.0216$ for all). Two-way Fe × Cu interactions were also noted for all measured parameters (as indicated in the individual panels). Since significant 2-way interactions were noted, Tukey's multiple comparisons post hoc test was utilized to determine differences among individual groups for each parameter; labeled means without a common letter differ ($P < 0.05$).

Table 6. *Selected dietary iron overload studies*

PMID	Dietary Fe, %	Age	Rodent (Strain)	Weeks on Diet	BW	Hb	Liver Fe	Serum Fe
8915458	2	Weanling	Rat (Wistar)	8–10	NC	NM	Up	Up
25956034	0.84	Adult (20 g)	Mouse (C57BL/6)	16	Down	NC	NM	NM
23578384	3	6-wk	Mouse (C57BL/6)	16	Down	NM	NM	Up
10656628	1–2	Adolescent	Rat (F344)	5	Down	NM	NM	NM
10207812	1.25–2.5	Weanling	Rat (Wistar)	30	Down	NM	Up	NM
21826460	2–3	Weanling	Rat (Sprague-Dawley)	3	Down	Up	Up	NM
7705783	3	Weanling	Rat (Porton)	10	Down	NM	Up	NM
24465846	2	Weanling	Rat (Sprague-Dawley)	3	Down	NC	Up	NM

PMID, PubMed ID; BW, body weight; Hb, hemoglobin; NC, no change; NM, not measured.

Downloaded from http://ajpgi.physiology.org/ by 10.220.33.6 on November 6, 2017

DISCLOSURES

No conflicts of interest, financial or otherwise, are declared by the authors.

AUTHOR CONTRIBUTIONS

J.-H.H. and J.F.C. conceived and designed research; J.-H.H. and C.D. performed experiments; J.-H.H. analyzed data; J.-H.H., C.D., and J.F.C. interpreted results of experiments; J.-H.H. prepared figures; J.-H.H. and J.F.C. drafted manuscript; J.-H.H., C.D., and J.F.C. edited and revised manuscript; J.-H.H., C.D., and J.F.C. approved final version of manuscript.

REFERENCES

1. **Bellier S, Da Silva NR, Aubin-Houzelstein G, Elbaz C, Vanderwinden JM, Panthier JJ.** Accelerated intestinal transit in inbred mice with an increased number of interstitial cells of Cajal. *Am J Physiol Gastrointest Liver Physiol* 288: G151–G158, 2005. doi:10.1152/ajpgi.00048.2004.
2. **Brissot P, Guyader D, Loréal O, Lainé F, Guillygomarc'h A, Moirand R, Deugnier Y.** Clinical aspects of hemochromatosis. *Transfus Sci* 23: 193–200, 2000. doi:10.1016/S0955-3886(00)00088-6.
3. **Collins JF, Franck CA, Kowdley KV, Ghishan FK.** Identification of differentially expressed genes in response to dietary iron deprivation in rat duodenum. *Am J Physiol Gastrointest Liver Physiol* 288: G964–G971, 2005. doi:10.1152/ajpgi.00489.2004.
4. **Collins JF, Prohaska JR, Knutson MD.** Metabolic crossroads of iron and copper. *Nutr Rev* 68: 133–147, 2010. doi:10.1111/j.1753-4887.2010.00271.x.
5. **Fox PL.** The copper-iron chronicles: the story of an intimate relationship. *Biometals* 16: 9–40, 2003. doi:10.1023/A:1020799512190.
6. **Frazer DM, Anderson GJ.** Iron imports. I. Intestinal iron absorption and its regulation. *Am J Physiol Gastrointest Liver Physiol* 289: G631–G635, 2005. doi:10.1152/ajpgi.00220.2005.
7. **Fuqua BK, Lu Y, Darshan D, Frazer DM, Wilkins SJ, Wolkow N, Bell AG, Hsu J, Yu CC, Chen H, Dunaief JL, Anderson GJ, Vulpe CD.** The multicopper ferroxidase hephaestin enhances intestinal iron absorption in mice. *PLoS One* 9: e98792, 2014. doi:10.1371/journal.pone.0098792.
8. **Gehrke SG, Kulaksiz H, Herrmann T, Riedel HD, Bents K, Veltkamp C, Stremmel W.** Expression of hepcidin in hereditary hemochromatosis: evidence for a regulation in response to the serum transferrin saturation and to non-transferrin-bound iron. *Blood* 102: 371–376, 2003. doi:10.1182/blood-2002-11-3610.
9. **Gulec S, Anderson GJ, Collins JF.** Mechanistic and regulatory aspects of intestinal iron absorption. *Am J Physiol Gastrointest Liver Physiol* 307: G397–G409, 2014. doi:10.1152/ajpgi.00348.2013.
10. **Gulec S, Collins JF.** Investigation of iron metabolism in mice expressing a mutant Menke's copper transporting ATPase (Atp7a) protein with diminished activity (Brindled; Mo (Br) (/y)). *PLoS One* 8: e66010, 2013. doi:10.1371/journal.pone.0066010.
11. **Gulec S, Collins JF.** Molecular mediators governing iron-copper interactions. *Annu Rev Nutr* 34: 95–116, 2014. doi:10.1146/annurev-nutr-071812-161215.
12. **Guo S, Frazer DM, Anderson GJ.** Iron homeostasis: transport, metabolism, and regulation. *Curr Opin Clin Nutr Metab Care* 19: 276–281, 2016. doi:10.1097/MCO.0000000000000285.
13. **Ha JH, Doguer C, Wang X, Flores SR, Collins JF.** High-iron consumption impairs growth and causes copper-deficiency anemia in weanling Sprague-Dawley rats. *PLoS One* 11: e0161033, 2016. doi:10.1371/journal.pone.0161033.
14. **Halfdanarson TR, Kumar N, Li CY, Phyliky RL, Hogan WJ.** Hematological manifestations of copper deficiency: a retrospective review. *Eur J Haematol* 80: 523–531, 2008. doi:10.1111/j.1600-0609.2008.01050.x.
15. **Hellman NE, Gitlin JD.** Ceruloplasmin metabolism and function. *Annu Rev Nutr* 22: 439–458, 2002. doi:10.1146/annurev.nutr.22.012502.114457.
16. **Klevay LM.** IHD from copper deficiency: a unified theory. *Nutr Res Rev* 29: 172–179, 2016. doi:10.1017/S0954422416000093.
17. **Klevay LM.** Iron overload can induce mild copper deficiency. *J Trace Elem Med Biol* 14: 237–240, 2001. doi:10.1016/S0946-672X(01)80009-2.
18. **Niederkofler V, Salie R, Arber S.** Hemojuvelin is essential for dietary iron sensing, and its mutation leads to severe iron overload. *J Clin Invest* 115: 2180–2186, 2005. doi:10.1172/JCI25683.
19. **Prohaska JR.** Impact of copper limitation on expression and function of multicopper oxidases (ferroxidases). *Adv Nutr* 2: 89–95, 2011. doi:10.3945/an.110.000208.
20. **Ranganathan PN, Lu Y, Fuqua BK, Collins JF.** Discovery of a cytosolic/soluble ferroxidase in rodent enterocytes. *Proc Natl Acad Sci USA* 109: 3564–3569, 2012. doi:10.1073/pnas.1120833109.
21. **Ranganathan PN, Lu Y, Jiang L, Kim C, Collins JF.** Serum ceruloplasmin protein expression and activity increases in iron-deficient rats and is further enhanced by higher dietary copper intake. *Blood* 118: 3146–3153, 2011. doi:10.1182/blood-2011-05-352112.
22. **Ravia JJ, Stephen RM, Ghishan FK, Collins JF.** Menkes Copper ATPase (Atp7a) is a novel metal-responsive gene in rat duodenum, and immunoreactive protein is present on brush-border and basolateral membrane domains. *J Biol Chem* 280: 36221–36227, 2005. doi:10.1074/jbc.M506727200.
23. **Rishi G, Wallace DF, Subramaniam VN.** Hepcidin: regulation of the master iron regulator. *Biosci Rep* 35: e00192, 2015. doi:10.1042/BSR20150014.
24. **Shankaran K, Gill HH, Desai HG.** Genetic hemochromatosis presenting as asymptomatic hepatomegaly. *Indian J Gastroenterol* 13: 64–65, 1994.
25. **US Environmental Protection Agency.** *Acid Digestion of Sludges, Solids and Soils*. Cincinnati, OH: Office of Solid and Hazardous Wastes. 1996, SW-846, part 1.
26. **Wilkins SJ, Frazer DM, Millard KN, McLaren GD, Anderson GJ.** Iron metabolism in the hemoglobin-deficit mouse: correlation of diferric transferrin with hepcidin expression. *Blood* 107: 1659–1664, 2006. doi:10.1182/blood-2005-07-2614.

Downloaded from http://ajpgi.physiology.org/ by 10.220.33.6 on November 6, 2017